ORIGINAL ARTICLE

Pyrolysed almond shells used as electrodes in microbial electrolysis cell

Cristian Arenas[1] · Ana Sotres[1] · Raúl M. Alonso[1] · Judith González-Arias[1] · Antonio Morán[1] ·
Xiomar Gómez[1]

Abstract

The large cost of components used in microbial electrolysis cell (MEC) reactors represents an important limitation that is delaying the commercial implementation of this technology. In this work, we explore the feasibility of using pyrolysed almond shells (PAS) as a material for producing low-cost anodes for use in MEC systems. This was done by comparing the microbial populations that developed on the surface of PAS bioanodes with those present on the carbon felt (CF) bioanodes traditionally used in MECs. Raw almond shells were pyrolysed at three different temperatures, obtaining the best conductive material at the highest temperature (1000 °C). The behaviour of this material was then verified using a single-chamber cell. Subsequently, the main test was carried out using two-chamber cells and the microbial populations extant on each of the bioanodes were analysed. High-throughput sequencing of the 16S rRNA gene for eubacterial populations was carried out in order to compare the microbial communities attached to each type of electrode. The microbial populations on each electrode were also quantified by real-time polymerase chain reaction (real-time PCR) to determine the amount of bacteria capable of growing on the electrodes' surface. The results indicated that the newly developed PAS bioanodes possess a biofilm similar to those found on the surface of traditional CF electrodes.

Keywords Microbial electrolysis cells · Bioanodes · Biomass pyrolysis · Electrodes

1 Introduction

The ever-increasing demand for energy, as well as associated environmental problems (such as water pollution and depletion of resources), has led to an intensive search for renewable energy sources and processes capable of generating green materials. The advances achieved in these research fields have important applications in the efficient management of wastewater treatment plants, leading to the development of a variety of novel treatment strategies. Bioelectrochemical systems (BES), more specifically microbial electrolysis cells (MECs), represent promising technologies with applications in wastewater treatment and in the recovery of resources [1]. MEC operation is based on the oxidation of organic compounds, a process catalysed by microorganisms capable of transferring electrons to a solid element, the anode. The electric current thus generated has an important role in reduction reactions taking place in the cathode, which is the counter electrode. The cathodic reaction allows the production of valuable chemicals like methane, ethanol and hydrogen, as long as a certain potential is applied. This potential is necessary for pumping the electrons from the anode to the cathode. One key element that contributes to both the efficiency and cost of MEC systems is the anode, due to its relatively high cost and its influence on the current density. This fact has led to numerous studies focused on the development of new and cheaper anode materials [2–4].

Ideal electrodes for use in BES should possess high conductivity, good biocompatibility, good chemical stability, a large surface area and reasonable pore distribution and should be low cost [5]. The use of carbonaceous materials as anodes has been extensively explored, as they meet most of these requirements. These carbon-based materials include graphite rods, carbon brushes, carbon cloth, carbon paper and carbon

✉ Xiomar Gómez
xagomb@unileon.es

[1] Chemical and Environmental Bioprocess Engineering Group, Natural Resources Institute (IRENA), Universidad de León, Av. de Portugal 41, 24009 León, Spain

felt (CF). All of these materials possess good conductivity and biocompatibility [6]. While the cost of electrodes is not often an issue in small-scale MECs, it represents a barrier that can limit the large-scale implementation of this technology. It is estimated that the cost of the anode can be as high as 20–50% of the total BES cost [7]. Reducing the cost while maintaining the properties that make these materials useful in BES is crucial in order to ensure that industrial applications are cost-effective [8].

Recently, biomass-derived products have been evaluated as an alternative to traditional electrodes. They are low cost and possess an inherent porous architecture, good biocompatibility and eco-friendly properties [9], making them ideal for applications such as electrochemical storage systems [3] and BES [10, 11]. A number of successful examples of using these materials for these applications exist. Chen et al. [12] tested the use of chestnut shell and reported that this material increased the power output 2.3-fold as compared with carbon cloth anodes in microbial fuel cells (MFCs). Huggins et al. [13] evaluated the effect of using wood-derived biochar as cathode and anode material in an MFC on the treatment of wastewater and the recovery of nutrients. Their results showed that chemical oxygen demand (COD) removal was 95%, with an average reduction rate of 0.53 kg COD·m^{-3} d^{-1} in batch mode. Next, Chen et al. [14] evaluated the use of a three-dimensional macroporous kenaf anode. This material showed higher electrochemical activity and better performance than that of graphite rods. Zhang et al. [4] also compared the performance of a tubular bamboo charcoal with graphite rods and found that this biomass-derived material improved the power output by approximately 50%. Finally, Wei Chen et al. [15] prepared an anode from carbonized waste tire and obtained good results in an MFC achieving higher current density than when using a carbon felt electrode. Taken together, these findings clearly suggest that the carbonization of biomass is an effective method for producing conductive materials for use in low-cost electrodes.

The almond (*Prunus dulcis* L.) shell is an abundant by-product from the almond processing industry and represents an abundant renewable resource in almond-producing countries such as Spain [16] and the USA [17]. The worldwide annual mean production of almonds is estimated at 1.97 million tons (MT), while Spain alone produces approximately 196,700 tons. This translates to between 0.68 and 1.47 MT of almond shells annually. As such, this material is an accessible and low-cost biomass that can be converted into conductive material via an activation process.

To our knowledge, the evolution of active and non-active microbial populations in this type of low-cost electrodes and the influence on the functioning of an MEC has not been studied yet. Therefore, the main objective of this work was to evaluate the feasibility of using pyrolysed almond shell (PAS) as a low-cost anode in an MEC. The experimental work

proposed also intends an evaluation of bacterial populations growing in biofilms formed in anodes based on low-cost materials and those formed in commonly used anodes in bioelectrochemical systems as it is carbon felt. The abundance of total bacteria and active bacteria present in the biofilm, as well as their taxonomic compositions, were compared between the PAS and CF bioanodes.

2 Materials and methodology

2.1 Working electrode preparation

Pyrolysis of raw almond shells was conducted in a semi-pilot scale rotatory tubular reactor (Nabertherm P300, Germany). Prior to the pyrolysis process, three holes were made in each half shell in order to allow electrical connection when used as an electrode. The temperature selected for the pyrolysis process was based on results reported in other works [18, 19] that showed that a temperature near 1000 °C reduces the oxygen/carbon (O/C) ratio and favours the presence of carbon bonds necessary for free electron movement. This fact was proven by preparing two other samples with a similar method but raising the samples to a lower final temperature [20]. The pyrolysis process applied to the almond shells was composed of three stages. In the first stage, a heating ramp of 5 °C min^{-1} was applied until reaching the final temperature (400, 600 and 1000 °C). Once this temperature was reached, the heat was held for 75 min (second stage), before cooling to room temperature (third stage). The PAS were subjected to a post-treatment in order to remove impurities and improve their hydrophilicity. The post-treatment consisted of consecutive immersion in a nitric acid solution (1 M, 30 min), acetone solution (1 M, 10 min) and ethanol solution (1 M, 10 min). Afterwards, the shells were immersed in deionized water and sonicated using an ultrasonic processor UP200S (Hielscher, Germany), which applied 57 W for 15 min (Fig. 1a).

2.2 MEC set-up and operation

A preliminary test was conducted for studying the suitability of PAS as electrode material for a bioanode. Once the PAS anode was operative, a second test was performed to compare its treatment capacity with that of a contrasting MEC system using a CF electrode as an anode.

The experiments were carried out using polycarbonate single-chambered MEC with dimensions of $50 \times 55 \times 55$ mm and an approximate volume per chamber of 80 mL. The cells were operated in a single chamber disposition, using a stainless steel mesh (AISI 304) as the counter and reference electrode and the corresponding anode (PAS or CF) as the working electrode (two electrodes mode). The projected area of the anode in these cells was 2.5 cm^2, while the cathode was

Fig. 1 **a** Conversion of raw almond shell to pyrolysed almond shell. **b** PAS ready to use as electrodes
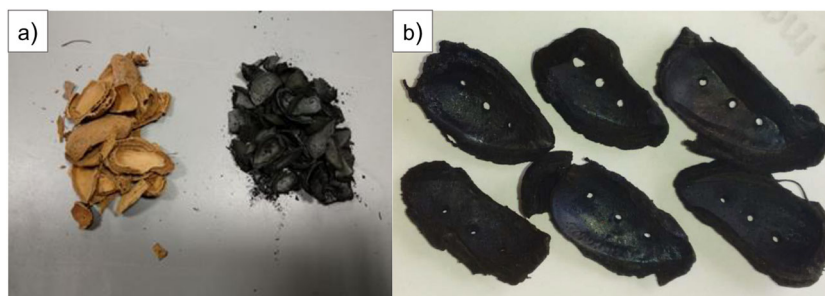
a stainless steel mesh (AISI 304) with an area of 5.1 cm^2. Titanium wire (Goodfellow, UK) was passed through the established holes of all electrodes (Fig. 1b). A power source applied a voltage of 1.0 V between the anode and cathode. The MECs were inoculated with a mixture of a wastewater-activated sludge (from the wastewater treatment plant located in León, Spain) and an effluent from other MECs that were operating in the lab for 6 months, to ensure the presence of an exoelectrogen microbiome. In each cycle, the feed was a synthetic solution (190 mL) that had the following composition (per litre): 0.87 g of K_2HPO_4, 0.68 g of KH_2PO_4, 0.25 g of NH_4Cl, 0.453 g of $MgCl_2 \cdot 6H_2O$, 0.1 g of KCl, 0.04 g of $CaCl_2 \cdot 2H_2O$, 10 mL of trace elements solution [21] and sodium acetate as a carbon source at a concentration of 683 mg·L^{-1}. The evolution of organic load during the experiments was followed through the total organic carbon (TOC) analysis, where the initial TOC was 200 mg·L^{-1}. Once the reactor was charged, it was then purged with N_2 for 20 min in order to remove the oxygen from the solution. The electrical conductivity of the initial anolyte solution was 4.32 mS cm^{-1} and the pH was adjusted to 7.0. A phosphate buffered saline solution (PBS; 0.1 M, pH 7.8) was used as the catholyte solution. The two initial MECs were operated for 2 months after the start-up period, which meant 17 regular cycles in batch mode.

In a subsequent test of MECs, two different types of electrodes were employed. Two cells used PAS and another used CF as the anode. The PAS anodes had the same characteristics previously described, while the latter had a projected area of 2.7 cm^2. The cells were denoted as PAS-MEC and CF-MEC based on the anode material used. The tests were conducted using two replicates of PAS-MEC. The cells used in this experiment are shown in Fig. 2. The experiments were carried out using polycarbonate double-chambered MECs with dimensions of $76 \times 81 \times 76$ mm and an approximate volume per chamber of 50 mL. The cells were operated in a two-electrode arrangement, using a stainless steel mesh (AISI 304) as the counter and reference electrode and the anode (PAS or CF) as the working electrode. A cation-exchange membrane (CMI-7000; Membranes International Inc., USA) was used for chamber separation. The cathodes of these cells and their connections were similar to those described for the preliminary experiment. MECs were inoculated and operated

under fed-batch conditions using an autoclaved synthetic solution, similar to previous tests. PAS-MEC and CF-MEC replicates were working for 94 days after start-up, providing 13 fed-batch cycles. The samples for microbiological analysis were taken from two anodes of PAS-MEC and CF-MEC at the end of the experiment.

2.3 Measurements and analytical determinations

Chemical structure and functional groups were elucidated by FTIR spectroscopy at three pyrolysis temperatures. A Thermo IS5 Nicolet (USA) spectrophotometer was used for obtaining FTIR spectra and acquired from 400 to 4000 cm^{-1} at room temperature (16 scans and spectral resolution of 4 cm^{-1}); the peak positions were determined using Origin 2015 software.

For the XRD analysis, the equipment used was a Scanning Electron Microscope JSM-6480LV, JEOL (Japan), with an X-ray microanalysis detector: ULTIM MAX, Oxford Instruments (UK). The software that allows one to take the photos and identify the elements is AZtec 4.0 SP2, Oxford Instruments (UK).

The voltage of the cells was maintained using an adjustable direct current (DC) power unit. The current data was acquired by a computer using an analogue output board (PCI-6713; National Instruments, Austin, TX). Current data was recorded at 12 min intervals. The effluents of the MECs were analysed by measuring the TOC content. This parameter was determined using a TOC analyser multi N/C 3100 (AnalytikJena, Germany). Coulombic efficiency (CE; %) is calculated as the ratio of electrons evacuated from the anode relative to the total electrons available from organic carbon oxidation.

2.4 Microbial community analyses

Once the second test was ended (two with PAS anodes and one with CF), the study of the microbial communities attached to the electrodes was performed. Pyrosequencing was utilized to sequence the 16S rRNA eubacterial gene for each anode type (PAS and CF), and this information was used to compare and contrast their microbial populations. The PAS electrode sample contained the populations from both PAS anodes. Genomic DNA and RNA were extracted from 150 to

Fig. 2 Experimental design with pyrolysed almond shell (PAS) and carbon felt (CF) as electrodes
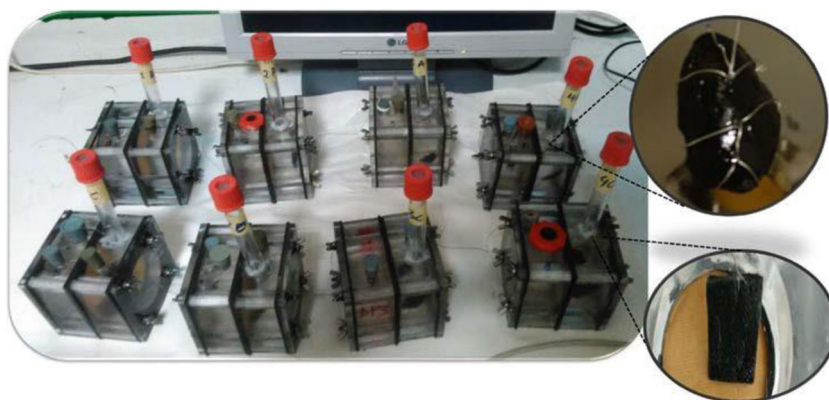
250 mg of each sample to be analysed. These samples included the inoculum used, as well as those obtained from the PAS and CF electrodes after 2 months of operation. A physical–chemical extraction protocol using bead-beating was performed using the PowerSoil® DNA isolation kit (MoBio Laboratories Inc., Carlsbad, CA, USA). The quality of the DNA extracts was tested using a 1% agarose gel dyed with GelRed™ nucleic acid gel stain. Extracted RNA was transformed to cDNA (complementary DNA synthesized from the messenger RNA (mRNA)), by reverse transcription polymerase chain reaction (RT-PCR), using the PrimeScript™ kit (Takara Bio Inc., Japan). The reaction was performed in a GeneAmp PCR System 9700 thermocycler (Applied Biosystems, USA). With both DNA and cDNA extracts obtained, massive sequencing was performed on these libraries. The 16S rRNA eubacterial gene was used to characterize the entire microbial community present in each sample. Illumina sequencing was carried out using a GS-FLX 454 sequencer (Roche, Switzerland) at the Molecular Research DNA Laboratory (Shallowater, Texas, USA). Each sample was amplified with the 27Fmod primer (5′-AGRGTTTT GATCMTGCTCAG-3′) and 519R modBio primer (5′-GTNTTACNGCGGGKGCTG-3′). The PCR reaction was carried out in a GeneAmp PCR System 9700 thermocycler (Applied Biosystems, USA). The DNA readings obtained were compiled into FASTq files for computer processing. Later, the operational taxonomic units (OTUs) were taxonomically classified using the MOTHUR software (version 1.33.3) and the Ribosomal Database Project (https://rdp.cme.msu.edu/). The wealth and diversity indices were calculated using the MOTHUR (version 1.35.1) software and samples were normalized to the lowest number of sequences.

An RT-PCR analysis of the 16S rRNA gene was also performed to quantify the total populations of eubacteria attached to both electrodes at the end of the experiments. Quantitative PCR (qPCR) analyses were performed on both DNA and cDNA samples. The set of primers used was 314F qPCR (5′-CCTACGGGGAGGCAGCAGCAG-3) and 518R qPCR
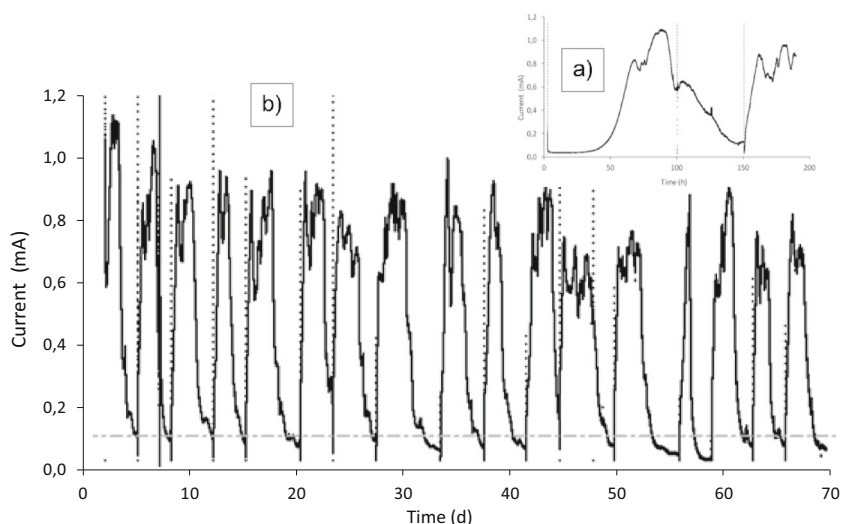
(5′-ATTACCGGGGCTGGCTGGG-3′). The thermocycler used was StepOne Plus Real-Time PCR System (Applied Biosystems, USA) and the results were processed with the same software as this equipment.
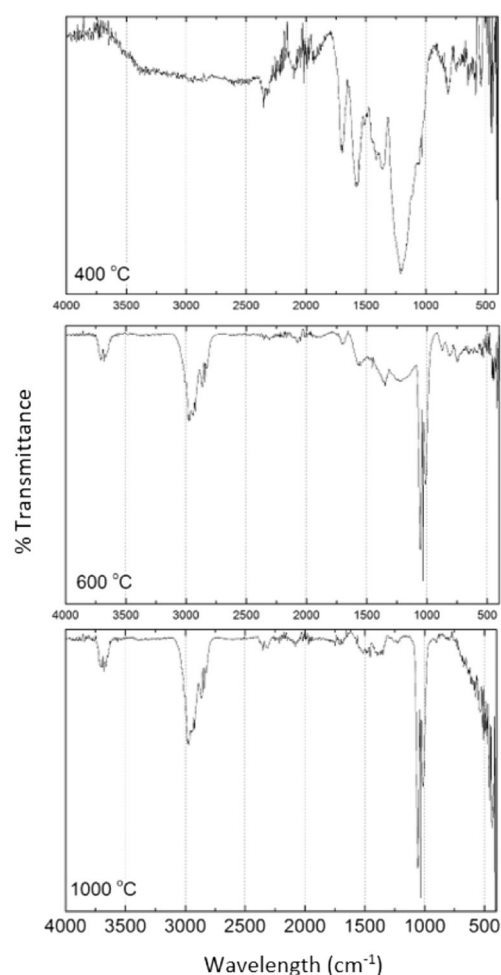
Fig. 3 FTIR spectra (4000–400 cm^{-1}) of biochars produced at three different temperatures

3 Results

3.1 Material preparation

The results of the XRD show, as expected, a greater oxygen loss as the final pyrolysis temperature increased, and at the same time, an enrichment of carbon that results in a graphitisation of the lignocellulosic material. At 400 °C, the O:C ratio is 32.5:65.5, at 600 °C, it is 14.8:79.5 and at 1000 °C it is 10.5:85.0 (Table S1). After pyrolysis, other elements such as Ca, K, Mg, Si, Al, P and Fe were detected in the biochar samples which is in accordance with results found in literature [22].

The chemical structure and functional groups were elucidated by FTIR spectroscopy at three pyrolysis temperatures (Fig. 3). A peak at 3600 cm^{-1} is ascribed to O–H stretching vibration with no hydrogen bond and is easier to find at higher temperatures, while the other O–H vibrations (3500–3200 cm^{-1}) appear in the biochar at 400 °C and disappear at higher temperatures. Signals between 3000 and 2800 cm^{-1} correspond to the C–H stretching band, and between 1475 and 1350 cm^{-1} to C–H deformation bands. Peaks between

1580 and 1675 cm^{-1} are related to C=C stretching vibrations and at 1300–1000 cm^{-1} they correspond to C–O stretching vibrations. The band around 1045 cm^{-1} is associated with the vibration of C–O–C links that is clear at the highest temperatures and is related to the decrease in the O/C ratio and the loss of oxygenated functional groups.

The resistivity of PAS was measured with the voltage probes. This value was found to be between 1.5×10^{-3} and 2×10^{-3} Ω m of resistivity for PAS at 1000 °C, which is about the same order of magnitude as the CF resistivity, at 3×10^{-3} Ω m. The resistivity of PAS produced at 400 and 600 °C was greater than 10 Ω m. These results confirm that the development of electrogenic biofilms in materials produced at 1000 °C could be enhanced because of the greater capacity of this material to evacuate the electric current.

3.2 Preliminary experiments

In each cycle, the current produced was recorded and the acetate degradation was evaluated in terms of TOC removal. The first cycle (Fig. 4a) shows the typical lag phase (~30 h) followed by the exponential growth phase. This first cycle

Fig. 5 Current density profiles of PAS-MEC and CF-MEC in experiments using polycarbonate double-chambered MECs
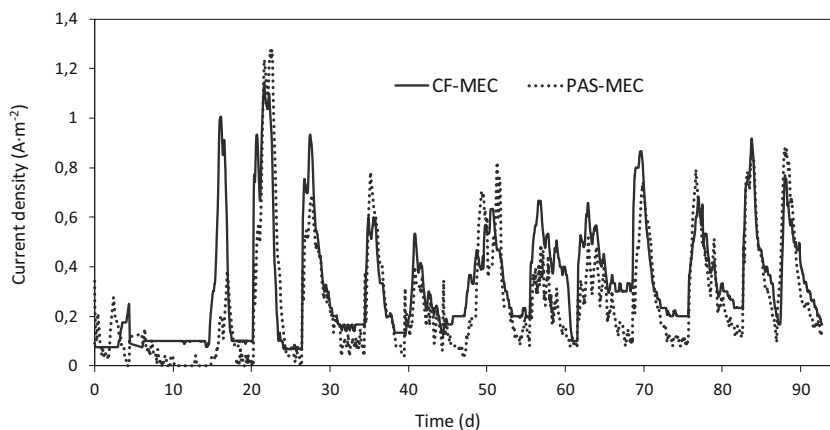
Table 1 Parameters of PAS-MEC and CF-MEC performance experiments

Parameter	Pyrolysed almond shell (PAS)	Carbon felt (CF)
Organic matter removal (%)	91.5 ± 6.2	93.0 ± 4.9
Coulombic efficiency (%)	62–85	64–79
Average current density (A m^{-2})	1.8 ± 0.4	1.9 ± 0.3

Table 2 Characteristics of the sequences obtained for the analysis of microbial populations

Sample	Number of reads	Mean length (bp)
Inoculum (sludge)	74,124	492.5
PAS (DNA)	41,750	500.4
PAS (cDNA)	49,681	516.4
CF (DVA)	63,096	492.3
CF (cDNA)	47,341	517.0

includes the initial development of an anodic biofilm, which stabilizes its growth during the beginning of the second cycle and can be observed in the following cycles (Fig. 4b). This fact can be deduced from the mean slope at the beginning of each cycle, which is very sharp (step response) from the third cycle onwards. The coulombic efficiencies were between 66 and 82%, and the average current obtained was 0.74 ± 0.09 mA. The maximum current density was 1.7 A m^{-2} with respect to the surface of the projected area of the anode, a value that could be considered as within a normal range for anodic mixed biofilms dominated by *Geobacter* species. After 30 days, at the end of each cycle, the organic matter degradation was complete in the two cells, yielding an average TOC removal rate of 50 ± 10 mg·L^{-1} d^{-1}. The results of these preliminary tests confirmed the viability of PAS as the working electrode in BES. The current densities and the ohmic resistances obtained indicate that the performance of these materials is comparable to the typical carbon materials used in BES, such as CF.

3.3 PAS-MEC and CF-MEC performance

Once the possibility of using PAS as a BES electrode had been demonstrated, the subsequent stage involved the comparison between the PAS and a conventional carbon-based electrode. The surface characteristics of the PAS [17] make the CF a suitable benchmark material. The PAS-MEC and the CF-MEC were run for 13 fed-batch cycles. Overall, the behaviour of the two cells was similar except with regard to the establishment of system stability in the initial cycles. This was due to differences in the placement of the membranes. On average, each fed-batch cycle took 5 days to complete. It should be noted that in the intermediate cycles, there were some problems due to power outages in the lab (Fig. 5). For this reason, cycles 6, 8 and 9 were not taken into account in the calculation of efficiencies. The highest density peak was reached by PAS-MEC with a value near 3.5 A m^{-2} and an average current density close to 2 A m^{-2}. Figure 5 shows that in the start-up (first 2 cycles), there were differences between the cells. In the following cycles, a very similar trend and behaviour is shown. The coulombic efficiencies were between 62 and 85% for PAS-MEC and 64 and 79% for CF-MEC (Table 1). These values indicate a high efficiency in the organic matter conversion through exoelectrogenic bacteria. The organic matter removal in each cycle is near 90% (Table 1) for both types of electrodes. These results demonstrate that using PAS electrodes as bioanodes results in similar values to those obtained from the CF-MEC bioanodes.

Fig. 6 Number of 16S rRNA gene copies obtained from DNA and cDNA samples
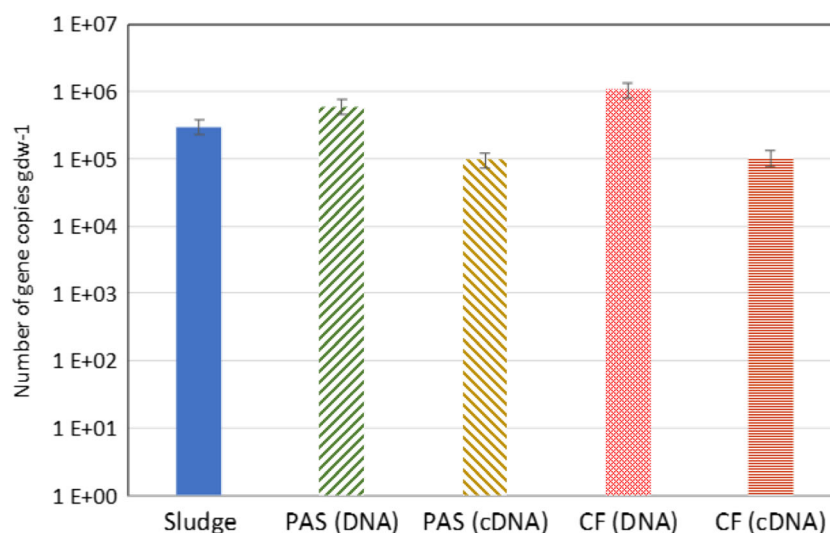
Table 3 Richness and diversity index at the genus level

Sample	Shannon	Inv Simpson	Fisher Alpha	OBS	Chao1	ACE
Inoculum (sludge)	3.84	19.2	63.0	446	560.7	556.9
PAS (DNA)	3.06	10.9	29.8	216	279.2	280.9
PAS (cDNA)	2.98	6.7	38.7	277	326.5	326.8
CF (DNA)	3.28	10.7	42.9	313	403.2	385.1
CF (cDNA)	2.47	4.8	32.5	237	314.4	333.8

3.4 Microbial community analysis

At the end of the last cycle, samples were taken from the bioanodes to characterize the microbial populations attached to the electrodes. The numbers of total bacteria (DNA) and active bacteria (cDNA) were quantified by qPCR of the 16S rRNA gene (Fig. 6) to determine the amount of bacteria present in the biofilm. The amount of bacteria present in the sewage sludge used as inoculum was also quantified, showing the increase in the total number of gene copies per gram in the MECs. Comparisons were made between the bioanodes from PAS-MEC and CF-MEC. The number of gene copies was higher in the sample from CF-MEC than PAS-MEC, which was supported by a very close ratio between cDNA and DNA. The ratios between active and total bacteria were approximately 15% and 10% for the PAS and CF samples, respectively.

There are differences in the amount of total bacteria present in each of the biofilms. However, the active populations are of the same order of magnitude for both electrodes (Fig. 6), which explains why the current densities reached at the end of the experiment are very similar for both reactors. While the initial bacterial growth is faster in the CF-MEC sample, the populations appear to equalize

over time (Fig. 5). Table 2 contains data on the number of reads and the mean length of the sequenced fragments (base pairs) of each sample. The number of successful reads was between 41,750 and 74,124, with an average length of 492 to 517 base pairs. Based on these results, the sequencing data is of good quality and is suitable for further analysis.

The indices of richness and diversity were calculated to compare the microbial population structure in both electrodes with respect to those initially present in the inoculum sample, as well as to be able to compare results between electrodes at the end of the experiment. The diversity indices calculated were Shannon, Inv Simpson and Fisher Alpha, while the richness estimators were the observed OTUs (OBS), Chao1 and ACE.

The results showed that the sewage sludge has higher indices of both richness and diversity than the electrode samples (Table 3), as would be expected. Richness and diversity were reduced in all bioanode samples due to specialization of the microbial populations. Likewise, it was observed that the diversity was lower in the active populations (cDNA) compared to those from the total populations (DNA). Finally, there are no large differences in the richness or diversity of the electrode samples, but there is a greater DNA richness in CF than

Fig. 7 Taxonomic classification at the phylum level obtained by massive sequencing of the 16S rRNA gene. Groups accounting for less than 1% of the total number of sequences per sample are classified as "Others"
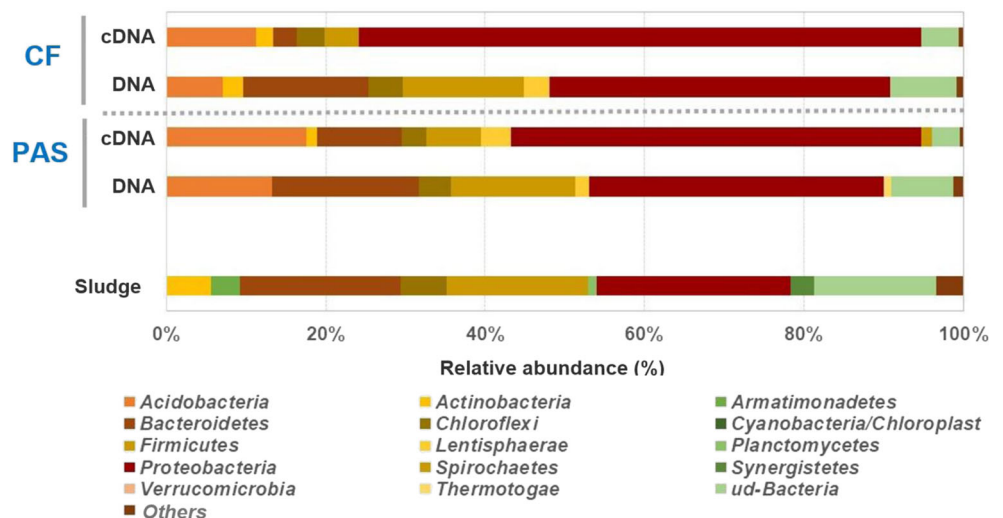
Fig. 8 Taxonomic classification at the genus level obtained by massive sequencing of the 16S rRNA gene. The numbers over the columns are the sum of the genera boxed in the legend
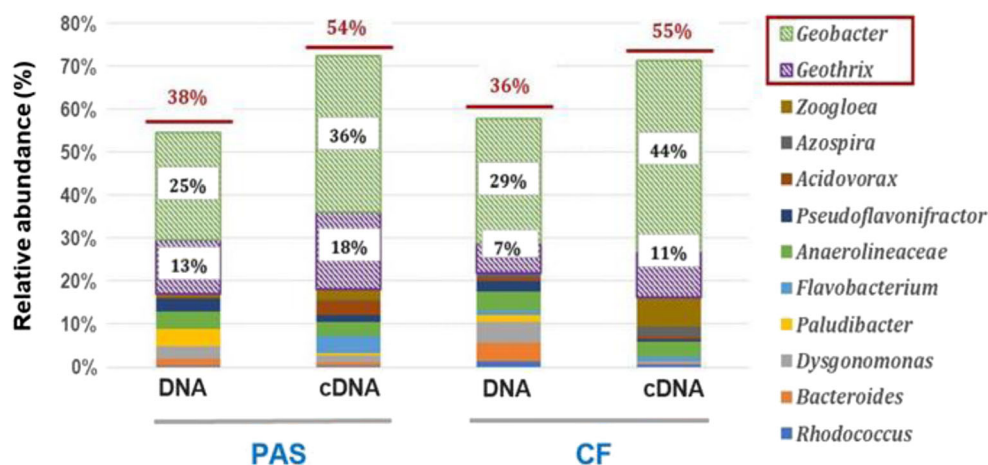
PAS, in line with a greater number of reads. The richness in cDNA is similar for PAS and CF, indicating the similar behaviour of both types of electrodes.

The composition of the eubacterial community in the sludge was analysed in depth in order to acquire information about the microbiological relationships related to the functioning of the reactors. At the phylum level (Fig. 7), the Proteobacteria group is the most abundant in the electrodes and is the dominant phylum in all samples. Compared to a 24.4% abundance in the inoculum, this group accounts for 37.0% to 71.0% of the anodic samples. This phylum, one of the most relevant in the BES [23], has several exoelectrogenic bacteria. Another phylum enriched in the electrodes that was not identified in the inoculum was Acidobacteria, with an abundance of 7 to 18%. This group has some functional connections with Acidobacteria and Actinobacteria in MFCs [24].

Figure 8 depicts the main genus identified in the PAS and CF electrodes in terms of relative abundance. As seen in Fig. 6, the abundance of the gene copy number of the 16S rRNA gene in the active populations (cDNA) was an order of magnitude below that of the total populations (DNA). However, the relative abundance of the two main genera was above the value for the active microbial community (cDNA). These two genera are *Geobacter* and *Geothrix*, which were identified in both DNA and cDNA samples, increasing their abundance from 36 to 38% in the total community to 54 to 55% in the active community (Fig. 8). Both genera are well-known electroactive microorganisms that are mainly responsible for organic matter oxidation, with acetate being one of its preferable substrates. The presence of these genera in the PAS-MECs is indicative of the suitability of this material for bioelectrochemistry applications. Therefore, there are no major differences in the amount of bacteria capable of growing on the surface of either electrode, nor in the genera of dominant bacteria. These results agree with those obtained in terms of reactor yields, where the organic

matter degradations, coulombic efficiencies and current densities recorded at the end of the experiments were similar for both CF-MEC and PAS-MEC conditions. They also agree with the results reported by Martínez et al. [25], who evaluated the microbial communities in an anaerobic digester supplemented with biochar. These authors reported that the addition of this carbon-conductive material favoured the development of electroactive microorganisms, which resulted in an improvement of the digestion performance. These results support the production of low-cost biochar-based electrodes, as proposed by Mian et al. [26], for reducing the capital investment required for bioelectrochemical systems and illustrate an example of the actual effect of biochar on the environment [27].

4 Conclusions

The results of this research demonstrate that the use of pyrolysed almond shells in the production of sustainable and cost-effective electrodes for bioelectrochemical systems is feasible, as they perform comparably to carbon felt electrodes. The results of the microbiological study revealed a similar structure and taxonomic composition between the PAS electrode and the CF electrode, confirming the good electrical connection bacteria-electrode and increasing the electron transfer efficiency between microorganisms and the low-cost material. These results demonstrate the suitability of using PAS as anode material in MECs.

References

1. Escapa A, Mateos R, Martínez EJ, Blanes J (2016) Microbial electrolysis cells: an emerging technology for wastewater treatment and energy recovery. From laboratory to pilot plant and beyond. Renew Sust Energ Rev 55:942–956. https://doi.org/10.1016/j.rser.2015.11.029

2. Hegab HM, ElMekawy A, van den Akker B et al (2018) Innovative graphene microbial platforms for domestic wastewater treatment. Rev Environ Sci Biotechnol 17:147–158. https://doi.org/10.1007/s11157-018-9459-0

3. Sonawane JM, Yadav A, Ghosh PC, Adeloju SB (2017) Recent advances in the development and utilization of modern anode materials for high performance microbial fuel cells. Biosens Bioelectron 90:558–576. https://doi.org/10.1016/J.BIOS.2016.10.014

4. Zhang J, Li J, Ye D et al (2014) Tubular bamboo charcoal for anode in microbial fuel cells. J Power Sources 272:277–282. https://doi.org/10.1016/j.jpowsour.2014.08.115

5. Thambidurai A, Lourdusamy JK, John JV, Ganesan S (2014) Preparation and electrochemical behaviour of biomass based porous carbons as electrodes for supercapacitors - a comparative investigation. Korean J Chem Eng 31:268–275. https://doi.org/10.1007/s11814-013-0228-z

6. Mohanakrishna G, Kalathil S, Pant D (2017) Reactor design for bioelectrochemical systems. In: Microbial fuel cell: a bioelectrochemical system that converts waste to Watts. Springer International Publishing, New York, pp 209–227

7. Rozendal RA, Hamelers HVM, Rabaey K, Keller J, Buisman CJ (2008) Towards practical implementation of bioelectrochemical wastewater treatment. Trends Biotechnol 26:450–459. https://doi.org/10.1016/J.TIBTECH.2008.04.008

8. Maksimova YG (2019) Microorganisms and carbon nanotubes: interaction and applications (review). Appl Biochem Microbiol 55:1–12. https://doi.org/10.1134/S0003683819010101

9. Pandey G (2019) Biomass based bio-electro fuel cells based on carbon electrodes: an alternative source of renewable energy. SN Appl Sci 1:1–10. https://doi.org/10.1007/s42452-019-0409-4

10. Chen J, Zhou X, Mei C et al (2017) Evaluating biomass-derived hierarchically porous carbon as the positive electrode material for hybrid Na-ion capacitors. J Power Sources 342:48–55. https://doi.org/10.1016/j.jpowsour.2016.12.034

11. Momodu D, Madito M, Barzegar F, Bello A, Khaleed A, Olaniyan O, Dangbegnon J, Manyala N (2017) Activated carbon derived from tree bark biomass with promising material properties for supercapacitors. J Solid State Electrochem 21(3):859–872. https://doi.org/10.1007/s10008-016-3432-z

12. Chen Q, Pu W, Hou H, Hu J, Liu B, Li J, Cheng K, Huang L, Yuan X, Yang C, Yang J (2018) Activated microporous-mesoporous carbon derived from chestnut shell as a sustainable anode material for high performance microbial fuel cells. Bioresour Technol 249:567–573. https://doi.org/10.1016/J.BIORTECH.2017.09.086

13. Huggins T, Wang H, Kearns J et al (2014) Biochar as a sustainable electrode material for electricity production in microbial fuel cells. Bioresour Technol 157:114–119. https://doi.org/10.1016/j.biortech.2014.01.058

14. Chen S, He G, Hu X, Xie M, Wang S, Zeng D, Hou H, Schröder U (2012) A three-dimensionally ordered macroporous carbon derived from a natural resource as anode for microbial bioelectrochemical systems. ChemSusChem 5:1059–1063. https://doi.org/10.1002/cssc.201100783

15. Chen W, Feng H, Shen D, Jia Y, Li N, Ying X, Chen T, Zhou Y, Guo J, Zhou M (2018) Carbon materials derived from waste tires as high-performance anodes in microbial fuel cells. Sci Total Environ 618:804–809

16. Queirós CSGP, Cardoso S, Lourenço A, Ferreira J, Miranda I, Lourenço MJV, Pereira H (2019) Characterization of walnut, almond, and pine nut shells regarding chemical composition and extract composition. Biomass Convers Biorefinery 10:175–188. https://doi.org/10.1007/s13399-019-00424-2

17. Aktas T, Thy P, Williams RB et al (2015) Characterization of almond processing residues from the Central Valley of California for thermal conversion. Fuel Process Technol 140:132–147. https://doi.org/10.1016/j.fuproc.2015.08.030

18. Feng H, Jia Y, Shen D et al (2018) The effect of chemical vapor deposition temperature on the performance of binder-free sewage sludge-derived anodes in microbial fuel cells. Sci Total Environ 635:45–52. https://doi.org/10.1016/j.scitotenv.2018.04.124

19. Malika A, Jacques N, Fallah Jaafar E et al (2016) Pyrolysis investigation of food wastes by TG-MS-DSC technique. Biomass Convers Biorefinery 6(2):161–172. https://doi.org/10.1007/s13399-015-0171-9

20. Gupta S, Gupta GK, Mondal MK (2019) Slow pyrolysis of chemically treated walnut shell for valuable products: effect of process parameters and in-depth product analysis. Energy 181:665–676. https://doi.org/10.1016/j.energy.2019.05.214

21. Moreno R, San-Martín MI, Escapa A, Morán A (2016) Domestic wastewater treatment in parallel with methane production in a microbial electrolysis cell. Renew Energy 93:442–448. https://doi.org/10.1016/j.renene.2016.02.083

22. Gupta GK, Gupta PK, Mondal MK (2019) Experimental process parameters optimization and in-depth product characterizations for teak sawdust pyrolysis. Waste Manag 87:499–511. https://doi.org/10.1016/j.wasman.2019.02.035

23. San-Martín MI, Sotres A, Alonso RM, Díaz-Marcos J, Morán A, Escapa A (2019) Assessing anodic microbial populations and membrane ageing in a pilot microbial electrolysis cell. Int J Hydrog Energy 44(32):17304–17315. https://doi.org/10.1016/j.ijhydene.2019.01.287

24. Li X, Zhao Q, Wang X, Li Y, Zhou Q (2018) Surfactants selectively reallocated the bacterial distribution in soil bioelectrochemical remediation of petroleum hydrocarbons. J Hazard Mater 344:23–32. https://doi.org/10.1016/j.jhazmat.2017.09.050

25. Martínez EJ, Rosas JG, Sotres A et al (2018) Codigestion of sludge and citrus peel wastes: evaluating the effect of biochar addition on microbial communities. Biochem Eng J 137:314–325. https://doi.org/10.1016/j.bej.2018.06.010

26. Mian MM, Liu G, Fu B (2019) Conversion of sewage sludge into environmental catalyst and microbial fuel cell electrode material: a review. Sci Total Environ 666:525–539. https://doi.org/10.1016/j.scitotenv.2019.02.200

27. Wang JL, Wang SZ (2019) Preparation, modification and environmental application of biochar: a review. J Clean Prod 227:1002–1022. https://doi.org/10.1016/j.jclepro.2019.04.282